



UWS Academic Portal

DNA sequence-selective C8-linked pyrrolobenzodiazepine(PBD)-heterocyclic polyamide conjugates show anti-tubercular specific activities

Brucoli, Federico; D. Guzman, Juan; Basher, Mohammad A. ; Evangelopoulos, Dimitrios; McMahon, Eleanor; Munshi, Tulika; McHugh, Timothy D.; Fox, Keith R. ; Bhakta, Sanjib

Published in:
The Journal of Antibiotics

DOI:
[10.1038/ja.2016.43](https://doi.org/10.1038/ja.2016.43)

Published: 31/12/2016

Document Version
Peer reviewed version

[Link to publication on the UWS Academic Portal](#)

Citation for published version (APA):

Brucoli, F., D. Guzman, J., Basher, M. A., Evangelopoulos, D., McMahon, E., Munshi, T., McHugh, T. D., Fox, K. R., & Bhakta, S. (2016). DNA sequence-selective C8-linked pyrrolobenzodiazepine(PBD)-heterocyclic polyamide conjugates show anti-tubercular specific activities. *The Journal of Antibiotics*, 69, 843-849.
<https://doi.org/10.1038/ja.2016.43>

General rights

Copyright and moral rights for the publications made accessible in the UWS Academic Portal are retained by the authors and/or other copyright owners and it is a condition of accessing publications that users recognise and abide by the legal requirements associated with these rights.

Take down policy

If you believe that this document breaches copyright please contact pure@uws.ac.uk providing details, and we will remove access to the work immediately and investigate your claim.

1 **DNA sequence-selective C8-linked pyrrolbenzodiazepine(PBD)-heterocyclic polyamide**
2 **conjugates show anti-tubercular specific activities**

3 Federico Brucoli,^{1*} Juan D. Guzman,^{2,†‡} Mohammad A. Basher,^{4‡} Dimitrios Evangelopoulos,^{2,3‡}
4 Eleanor McMahon,² Tulika Munshi,^{2‡} Timothy D. McHugh,³ Keith R. Fox,⁴ and Sanjib Bhakta²

5 Author Affiliations

6 *¹School of Science, Institute of Biomedical and Environmental Health Research (IBEHR), University*
7 *of the West of Scotland, Paisley, PA1 2BE, Scotland, UK; ²Department of Biological Sciences,*
8 *Institute of Structural and Molecular Biology, Birkbeck College, University of London, London,*
9 *WC1E 7HX, UK; ³Centre for Clinical Microbiology, University College London, London, NW3 2PF,*
10 *UK; ⁴Centre for Biological Sciences, University of Southampton, Southampton SO17 1BJ, UK.*

11 *Corresponding author. Tel: +44-(0)141-848-3264; E-mail: federico.brucoli@uws.ac.uk

12 Present addresses:

13 †Departamento de Química y Biología, Universidad del Norte, Km 5 vía Puerto Colombia,
14 Barranquilla 081007, Colombia.

15 ‡The Francis Crick Institute, Mill Hill Laboratory, The Ridgeway, Mill Hill, London, NW7 1AA, UK.

16 ‡Institute of Infection and Immunity, St George's, University of London, Cranmer Terrace, London
17 SW17 0RE, UK.

18 ‡These two authors equally contributed to this study.

19

20

21

22 **Abstract**

23 New chemotherapeutic agents with novel mechanisms of action are in urgent need to combat the
24 tuberculosis pandemic. A library of twelve C8-linked pyrrolo[2,1-c][1,4]benzodiazepine(PBD)-
25 heterocyclic polyamide conjugates (**1-12**) was evaluated for anti-tubercular activity and DNA
26 sequence selectivity. The PBD-conjugates were screened against slow-growing *Mycobacterium bovis*
27 BCG and *M. tuberculosis* H₃₇Rv and fast-growing *Escherichia coli*, *Pseudomonas putida* and
28 *Rhodococcus sp.* RHA1 bacteria. DNase I footprinting and DNA thermal denaturation experiments
29 were used to determine the molecules' DNA recognition properties. The PBD-conjugates were highly
30 selective for the mycobacterial strains and exhibited significant growth inhibitory activity against the
31 pathogenic *M. tuberculosis* H₃₇Rv, with compound **4** showing MIC values (MIC = 0.08 mg/L) similar
32 to those of rifampin and isoniazid. DNase I footprinting results showed that the PBD-conjugates with
33 three heterocyclic moieties had enhanced sequence selectivity and produced larger footprints with
34 distinct cleavage patterns compared to the two-heterocyclic chain PBD-conjugates. DNA melting
35 experiments indicated a covalent binding of the PBD-conjugates to two AT-rich DNA-duplexes
36 containing either a central GGATCC or GTATAC sequence and showed that the polyamide chains
37 affect the interactions of the molecules with DNA. The PBD-C8-conjugates tested in this study have
38 a remarkable anti-mycobacterial activity and can be further developed as DNA-targeted anti-
39 tubercular drugs.

40 **Keywords**

41 Drug discovery; DNA-minor groove binding agents; Pyrrolobenzodiazepines; Anti-tubercular agents;
42 DNase I footprinting; *Mycobacterium tuberculosis*; HT-SPOTi

43 **1. Introduction**

44 Tuberculosis (TB) is a global health challenge, with 9 million new cases and 1.5 million deaths
45 reported in 2013.¹ Furthermore, it is estimated that one third of the world's population is infected
46 with *Mycobacterium tuberculosis*, accounting for a large reservoir of the bacilli.¹ The increasing
47 incidence of TB is also linked to the steady increase in multi-drug and extensively-drug resistant

48 tuberculosis (MDR/XDR-TB) strains, which renders TB difficult to treat.^{1,2} Therefore, new
49 antibiotics with novel and pleiotropic modes of action are urgently needed to combat the TB
50 pandemic, the rise of resistant bacilli and also provide new, safer and shorter drugs regimens. To this
51 end, the complete reconstruction of the *M. tuberculosis* regulatory network³ has laid the foundation
52 for the development of DNA-targeted anti-mycobacterial agents. The ability of DNA sequence-
53 selective agents to target specific promoter regions of the *M. tuberculosis* DNA can be exploited to
54 disrupt the binding of mycobacterial transcription factors, induce bacterial cell death, overcome
55 antimicrobial resistance and maximize therapeutic efficacy.

56 DNA-targeted chemotherapeutic agents are an important class of compounds, which have long
57 attracted interest due to their distinctive mode of action involving specific interactions with
58 predetermined DNA sequences.⁴⁻⁷ Among these agents, pyrrolo[2,1-*c*][1,4]benzodiazepines (PBDs)
59 have played a major role in cancer and antibacterial chemotherapy.^{8, 9} PBDs are a family of
60 antitumour-antibiotics first isolated from cultures of *Streptomyces* species.¹⁰ These molecules are
61 DNA sequence-selective agents that covalently bind, via their N10-C11 imine functionality, to the
62 C2-amino groups of guanine residues within the minor groove of DNA, spanning three DNA base
63 pairs with a preference for Pu-G-Pu (where Pu = purine; G = guanine) sequences (**Figure 1**).^{9,11}
64 PBD monomers block transcription by inhibiting RNA polymerase activity in a sequence-specific
65 manner.¹²

66 Since their discovery, several PBD analogues have been synthesised and extensively evaluated for
67 their anticancer and antibacterial activities.^{8, 13-17} However, to our knowledge, there are only few
68 studies focusing on the anti-mycobacterial activity of the PBDs. Taylor and Thurston reported that
69 PBD dimers, in which two PBD units are tethered through a C8/C8'' diether linker to improve DNA-
70 binding affinity and sequence specificity, exhibited notable activity against a panel of rapid and
71 relatively rapid-growing mycobacteria, *Mycobacterium smegmatis*, *M. fortuitum*, *M. abscessus*, *M.*
72 *phlei* and *M. aurum*.¹⁸ Although showing anti-mycobacterial activity, the PBD dimers displayed
73 significant cytotoxicity against human cell lines, especially compared to PBD monomers, and may be

74 only used as “drug of last resort” to treat intractable infections caused by multi-drug resistant
75 pathogens.¹⁹ In another study, Kamal *et al.* showed that PBD-5,11-diones (PBD dilactams) inhibited
76 the growth of *Mycobacterium avium*, *M. intracellulare* and *M. tuberculosis*. PBD-dilactams stabilise
77 duplex-DNA to a lesser extent than PBDs, as they lack the N10-C11 imine moiety responsible for the
78 electrophilic alkylation of the C2-NH₂ of guanine bases, thus resulting in a non-covalent DNA
79 interaction and reduced antibacterial and anticancer potency.^{9,20}

80 In the present study, we investigated the anti-mycobacterial activity and DNA binding properties of a
81 library of twelve C8-linked PBD-heterocyclic polyamide conjugates (**1-12**) (**Figure 2**), which were
82 previously shown to have strong *in vitro* anticancer activities.²¹⁻²³ The di- or tri-heterocyclic
83 polyamide chains of **1-12** are comprised of combinations of pyrrole (Py), imidazole (Im) and thiazole
84 (Th) rings known for their ability to modulate the ligands’ DNA-binding affinity.²⁴ C8-linked PBD-
85 polyamide conjugates, unlike PBD dilactams, retain the ability to form covalent DNA-adducts,
86 characteristic responsible for their improved cancer cell cytotoxicity and antibacterial activities,¹⁵ and
87 have a more favourable cytotoxicity profile compared to the PBD dimers.^{15,17}

88 PBD-conjugates **1-12** were screened against slow-growing *Mycobacterium bovis* BCG and *M.*
89 *tuberculosis* H₃₇Rv and fast-growing *Escherichia coli*, *Pseudomonas putida* and *Rhodococcus sp.* and
90 minimum inhibitory concentration values (MIC) were determined. Cytotoxicity against mouse
91 macrophages RAW264.7 was also evaluated. The DNaseI footprinting experiments and thermal
92 denaturation assays were used to evaluate the DNA recognition properties of **1-12**.

93 **2. Materials and methods**

94 *C8-linked PBD-heterocyclic polyamide conjugates*

95 The twelve PBD-conjugates **1-12** were synthesised and purified using published synthetic routes^{21,22}
96 and dissolved in DMSO prior to use.

97 *Microorganisms and mammalian cells*

98 *Mycobacterium bovis* BCG Pasteur (ATCC 35734) and *M. tuberculosis* H₃₇Rv (ATCC 27294), and
99 *Escherichia coli* K12 (ATCC 53323), *Pseudomonas putida* KT2442 (ATCC 47054) and *Rhodococcus*
100 *sp.* RHA1 were used to screen the antibacterial activity of the PBD conjugates. Murine macrophages
101 RAW264.7 (ATCC TIB71) were used in this study to evaluate the cytotoxicity of the PBD-
102 conjugates.

103 *Mammalian macrophage cytotoxicity assay using resazurin assay*

104 The quantitation of eukaryotic cell toxicity was carried out as previously described.²⁵

105 *Antibacterial assay against E. coli, P. putida and Rhodococcus sp.*

106 The evaluation of growth inhibition of the PDB-conjugates against *E. coli*, *P. putida* and *Rhodococcus*
107 *sp.* was performed using the spot culture growth inhibition assay (SPOTi) in 24 well plates.²⁶ A seed
108 culture of each bacteria was prepared in Luria Bertani (LB) broth and grown overnight at 37 °C with
109 shaking at 200 rpm. *Rhodococcus sp.* was grown in LB broth at 30 °C with shaking at 200 rpm.
110 Dilutions of the PBD-conjugates were performed in sterile DMSO at concentrations one thousand-
111 fold more concentrated than the concentrations to be tested. 2 µL of each dilution were dispensed in
112 each well of the 24 well plates, and 2 mL of LB agar were added to each well, and mixed. 2 µL of
113 each inoculum containing approximately 10⁵ colony-forming units (CFUs)/mL were carefully
114 dispensed into the middle of the well on the surface of the solidified agar. The plate was incubated
115 overnight at 37 °C for *E. coli* and *P. putida*, and at 30 °C for *Rhodococcus sp.* The plates were
116 visually inspected and minimum inhibitory concentrations (MIC) values were recorded as the lowest
117 concentration of PBD-conjugates where no growth was observed. Kanamycin was included as
118 positive control.

119 *Anti-mycobacterial screening using HT-SPOTi*

120 *M. bovis* BCG and *M. tuberculosis* H₃₇Rv were grown in Middlebrook 7H9 broth supplemented with
121 0.02% (v/v) glycerol, 0.05% (v/v) tween-80 and 10% (v/v) albumin, dextrose and catalase (ADC; BD

122 Biosciences) as a rolling culture at 2 rpm and 37 °C, and as a stand culture at 37 °C. The
123 antimycobacterial activities of the compounds were tested following the HT-SPOTi guidelines.^{26,27}
124 HT-SPOTi is a high-throughput growth inhibition assay conducted in a semi-automated 96 well plate
125 format. Compounds dissolved in DMSO at a final concentration of 50 mg/mL were serially diluted
126 and dispensed in a volume of 2 µL into each well of a 96 well plate to which 200 µL of Middlebrook
127 7H10 agar medium kept at 55 °C supplemented with 0.05% (v/v) glycerol and 10% (v/v) OADC was
128 added. Wells with no compounds (DMSO only) and isoniazid (positive control) were used as
129 experimental controls. To all the plates, a drop (2 µL) of mycobacterial culture containing 2×10^3
130 CFUs was spotted in the middle of each well and the plates were incubated at 37 °C for 7 days. The
131 MICs were determined as the lowest concentration of each compound where no mycobacterial growth
132 was observed.

133 *DNase I footprinting assay*

134 Footprinting reactions were performed as previously described²⁸ using the DNA fragments HexAfor
135 and HexBRev, which together contain all 64 symmetrical hexanucleotide sequences. The DNA
136 fragments were obtained by cutting the parent plasmids with *Hind*III and *Sac*I (*HexA*) or *Eco*RI and
137 *Pst*I (*HexBRev*) and were labelled at the 3'-end with [α -³²P]dATP using reverse transcriptase. After
138 gel purification the radiolabelled DNA was dissolved in 10 mM Tris-HCl pH 7.5 containing 0.1 mM
139 EDTA, at a concentration of about 10 c.p.s per µL as determined on a hand held Geiger counter. 1.5
140 µL of radiolabelled DNA was mixed with 1.5 µL ligand that had been freshly diluted in 10 mM Tris -
141 HCl pH 7.5, containing 10 mM NaCl. The complexes were left to equilibrate for at least 12 hours
142 before digesting with 2 µL DNase I (final concentration about 0.01 units/ml). The reactions were
143 stopped after 1 minute by adding 4 µL of formamide containing 10 mM EDTA and bromophenol blue
144 (0.1% w/v). The samples were then heated at 100 °C for 3 minutes before loading onto 8% denaturing
145 polyacrylamide gels containing 8 M urea. Gels were fixed in 10% acetic acid, transferred to 3MM
146 paper, dried and exposed to a phosphor screen overnight, before analysing with a typhoon
147 phosphorimager.

149 Fluorescence melting curves were determined in a Roche LightCycler, using a total reaction volume
150 of 20 μL . For each reaction the final oligonucleotide concentration was 0.25 μM , diluted in 10 mM
151 sodium phosphate pH 7.4 containing 100 mM NaCl. The experiments used the duplexes 5'-F-
152 AAAAGGATCCAAA/5'-TTTTGGATCCTTTT-Q and 5'-F-AAAAGTATACAAA/5'-
153 TTTTGTATACTTTT-Q (F = fluorescein and Q = dabcy). In a typical experiment the samples were
154 first denatured by heating to 95 $^{\circ}\text{C}$ at a rate of 0.1 $^{\circ}\text{C s}^{-1}$. The samples were then maintained at 95 $^{\circ}\text{C}$
155 for 5 min before annealing by cooling to 25 $^{\circ}\text{C}$ at 0.1 $^{\circ}\text{C s}^{-1}$ (this is the slowest heating and cooling
156 rate for the LightCycler). They were held at 25 $^{\circ}\text{C}$ for a further 5 min and then melted by heating to
157 95 $^{\circ}\text{C}$ at 0.1 $^{\circ}\text{C s}^{-1}$. Recordings of the fluorescence emission at 520 nm were taken during both the
158 melting steps as well as during annealing. The data were normalized to show the fractional change in
159 fluorescence for each sample between the starting and final values. T_m values were determined from
160 the first derivatives of the melting profiles using the Roche LightCycler software.

161 **3. Results**

162 *Growth inhibition of Mycobacterium spp.*

163 In **Table 1** are illustrated the results of the anti-tubercular and anti-bacterial screening, the
164 cytotoxicity evaluation and the selectivity index (SI) of **1-12**. Compounds **1-12** were tested for
165 growth inhibition against two slow-growing mycobacteria, *Mycobacterium bovis* BCG and *M.*
166 *tuberculosis* H₃₇Rv. The PBD-conjugates' MIC values against *M. tuberculosis* ranged from 0.08 to
167 5.19 mg/L, whereas the MIC values against *M. bovis* ranged from 0.04 to 20 mg/L. Dipyrrole-
168 including PBD-conjugate **4** (Py-Py-PBD) exhibited the highest growth inhibitory activity against *M.*
169 *tuberculosis* with a MIC value of 0.08 mg/L. Compounds **5** (Py-Py-Im-PBD), **7** (Im-Im-Py-PBD), **9**
170 (Py-Py-Th-PBD), **10** (Py-Th-Py-PBD) and **12** (Py-Py-Py-PBD) inhibited the growth of *M.*
171 *tuberculosis* at 0.16 mg/L concentration. PBD-conjugate **1** (Py-Th-PBD) was active against *M.*
172 *tuberculosis* and *M. bovis* at 0.31 and 0.16 mg/L, respectively, whereas compound **2** (Th-Py-PBD)

173 inhibited the growth of both mycobacteria at 0.63 mg/L. Compounds **6** (Py-Im-Py-PBD) and **8** (Im-
174 Im-Im-PBD) were found to be 60-fold more active against *M. tuberculosis* (0.32 mg/L) than *M. bovis*
175 BCG (20 mg/L), whereas PBD-conjugates **7**, **9** and **10** were two-fold more active against *M. bovis*
176 (0.08 mg/L) than *M. tuberculosis* (0.16 mg/L). Pyrrole-including PBD-conjugates **4** and **12** showed
177 the highest growth inhibitory activity against *M. bovis* with a MIC of 0.04 mg/L. On the other hand,
178 thiazole-including PBD-conjugates **3** (Th-Th-PBD) and **11** (Th-Th-Th-PBD) exhibited the lowest
179 growth inhibitory activity against both *M. tuberculosis* and *M. bovis* BCG with values of 5.19 and 20
180 mg/L, respectively. First-line anti-tubercular drugs isoniazid and rifampin were used as positive
181 controls and inhibited the growth of both mycobacterial strains at 0.05 mg/L.

182 *Antibacterial activity on E. coli* K12, *P. putida* KT2442 and *Rhodococcus sp.* RHA1

183 In order to evaluate the mycobacterial specificity of PBD-conjugates **1-12** in whole cell experiments
184 and determine whether the compounds selectively affected slow-growing mycobacteria in comparison
185 with fast-growing bacteria, we investigated the growth inhibitory activities of **1-12** against Gram-
186 positive *Rhodococcus sp.* RHA1 and Gram-negative *Escherichia coli* K12 and *Pseudomonas putida*
187 KT2442 bacteria. The results in **Table 1** show that the majority of PBD-conjugates (**1**, **4-7**, **9**, **10** and
188 **12**) had a significant growth inhibitory activity against *E. coli* and *Rhodococcus sp.* with a MIC value
189 of 1.25 mg/L. Interestingly, PBD-conjugate **8** was 150-fold more active against *M. tuberculosis* (0.32
190 mg/L) than Gram-negative *E. coli* and *P. putida* (>50 mg/L), whereas thiazole-containing PBD-
191 conjugates **3** and **11** were 10-fold more active against *M. tuberculosis* (5.19 mg/L) than *E. coli*, *P.*
192 *putida* and *Rhodococcus sp.* (>50 mg/L) strains. Tri-pyrrole-including PBD-conjugate **12** was active
193 against *P. putida* at 5 mg/L, whereas compounds **4** and **5** inhibited the growth of this bacterium at 10
194 mg/L. Compounds **7**, **9** and **10** were found to be approximately 300-fold more active against *M.*
195 *tuberculosis* (0.16 mg/L) than *P. putida* (50 mg/L). The aminoglycoside antibiotic kanamycin was
196 used as a positive control and inhibited the growth of *E. coli* and *P. putida* at 1.0 mg/L and
197 *Rhodococcus sp.* at 10 mg/L.

198

199 *Macrophage RAW264.7 cytotoxicity*

200 The PBD-conjugates displayed various degrees of cytotoxicity against mammalian macrophages
201 RAW264.7 with GIC₅₀ values ranging from 1.66 to 4.45 mg/L. The values of the Selectivity Index
202 (SI), which is the ratio between macrophage half-growth inhibition concentration (GIC₅₀) and MIC
203 against the virulent H₃₇Rv strain, ranged from 0.32 to 30.1, with PBD-conjugate **4** (Py-Py-PBD)
204 exhibiting the highest specificity (SI = 30.1) amongst the library members. PBD-conjugates **5**, **7**, **9**,
205 **10** and **12** exhibited a SI of 10.4, whereas **1** had a SI of 14.4. Thiazole-including PBD-conjugates **3**
206 and **11** showed the lowest specificity, with SI values of 0.46 and 0.32, respectively.

207 *DNase I footprinting*

208 DNase I footprinting was used to identify the binding sites of the PBD-conjugates, using the DNA
209 fragments HexAfor and HexBrev,²⁸ which together contain all 64 possible symmetrical
210 hexanucleotide sequences. The results are shown in **Figure 3**. The left hand panels show the
211 footprints with 10 µM of compounds **2**, **3**, **5**, **7**, **9** and **10** with HexAfor and HexBrev, while the two
212 panels on the right show examples of the concentration dependence of the footprints with **5** and **9** on
213 HexAfor. It is evident that compounds **5**, **9** and **10** produced large footprints in both HexAfor and
214 HexBrev, while compound **7** produced fewer footprints including two shorter footprints (4a and b)
215 within site 4. Each of these ligands produced a distinct cleavage pattern and the location of the major
216 footprints is indicated in **Figure 4**. All these compounds contain three rings conjugated to the PBD.
217 A few weaker footprints were seen with the compounds that only contain two conjugated rings.
218 Compound **2**, which contains thiazole and pyrrole rings, produced footprints at sites 2, 4 and 8, while
219 no footprints were seen with **3**, which contains two thiazole rings. It is clear that addition of the
220 heterocycles affects the interaction of PBD with DNA. PBD-conjugates **5** (Py-Py-Im-PBD), **9** (Py-
221 Py-Th-PBD) and **10** (Py-Th-Py-PBD) bound to sites 1, 2, 3 and 4 within HexBrev, and to sites 6, 7, 8
222 and 9 within HexAfor, while the footprint at site 5 in HexBrev is only evident with compounds **5** and
223 **9**. Compound **7** bound to fewer sites with clear footprints limited to sites 3, 4a and 4b on HexBrev
224 and site 8 on HexAfor. Although each ligand produced a characteristic cleavage pattern, it is

225 noticeable that many of the footprints contained a short A/T tract followed by a guanine. The two
226 right hand panels of **Figure 3** show the concentration dependence of the footprints with **5** and **9** on the
227 HexAfor fragment. At 5 μM concentration **5** produced a single footprint located in the lower part of
228 site 8 within the sequence 5'-GCGCTTAAGTACT. Compound **9** produced footprints that persisted
229 to lower concentrations, and the protections at the lower part of site 8 and in the centre of site 7 (5'-
230 TAAACGTT) were still evident with 0.5 μM ligand.

231 *DNA Melting Studies*

232 In order to further evaluate the contribution of the heterocyclic chains to the DNA recognition
233 properties of the PBD-conjugates, the effects of the ligands on DNA-melting temperature were
234 analysed using two fluorescently-labelled 14-mer DNA duplexes. These AT-rich DNA duplexes
235 contained either a central GGATCC or GTATAC and the results with 0.5 μM ligand are shown in
236 **Figure 5**. It can be seen that all four of these ligands stabilised the duplexes and produced transitions
237 at elevated temperatures. Since the ligands were covalently attached to the DNA, the T_m values of
238 each transition did not change with the ligand concentration. However, the relative proportions of the
239 different components were altered, so that a greater fraction of the higher T_m was evident with higher
240 ligand concentrations. Each of these duplexes contains more than one guanine with which the
241 conjugates could attach (two guanines for GTATAC and four for GGATCC) and further transitions
242 were observed at higher ligand concentrations, as evident for **10** with both oligonucleotide duplexes.
243 At a concentration of 0.5 μM the ligand was in excess of the target duplex (0.25 μM). The fraction of
244 the melting transition that has shifted to the higher temperature therefore indicates the proportion of
245 the duplex that has been modified within the incubation period, though the absolute values of the
246 melting transitions indicate the stabilization that is imparted by the bound ligand. The result of these
247 experiments are summarised in **Table 2**. It can be seen that there is a good correlation between the
248 large footprints produced by PBD-conjugates **9** and **10** with their greatest effect on the melting curves.
249 At 0.5 μM **9** shifted the entire melting curve to a higher temperature with both GTATAC ($\Delta T_m = 29$)
250 and GGATCC ($\Delta T_m = 35$) with a small amount of uncomplexed duplex (5 and 10%, respectively). A

251 similar effect is seen with **10** and GTATAC for which about 30% of the transition was shifted to an
252 even higher temperature transition. In contrast, a significant amount of uncomplexed duplex (25%)
253 was still evident with **10** and GGATCC, even though about 20% of the transition corresponded to a
254 higher transition that suggested binding of a second ligand. The melting curves with 0.5 μM **5** and **7**
255 contained a large amount of the transition that corresponded to the uncomplexed duplex. **5** and **7** had
256 a similar effect on GGATCC, though a greater fraction of GTATAC was bound by **7**.

257 **4. Discussion**

258 The anti-mycobacterial evaluation of PBD-conjugates **1-12** revealed that these compounds have
259 remarkable growth inhibitory activity against *M. tuberculosis* H₃₇Rv. The nature and the length of the
260 polyamide chain attached to the PBD unit had a significant influence on the molecules' anti-microbial
261 activity and DNA-sequence selectivity. The presence of pyrrole rings in the polyamide chains
262 affected the overall anti-tubercular activity of the compounds. The di-pyrrole-containing **4** had a MIC
263 value of 0.08 mg/L, which was comparable to those of isoniazid and rifampin, and an encouraging
264 therapeutic window (SI = 30) that could be further improved in the second generation of PBD-based
265 anti-tuberculosis agents. **Although displaying some degrees of cytotoxicity towards mammalian cells,**
266 **PBD-conjugate 4 represents a promising anti-TB therapeutic lead, particularly in light of the results**
267 **generated by the large TB drug discovery campaign recently conducted by GlaxoSmithKline (GSK).²⁹**
268 **Researchers at GSK screened a 2 million proprietary-compounds collection for anti-mycobacterial**
269 **activity against *M. tuberculosis* H37Rv and for cytotoxicity against mammalian cells (HepG2). A set**
270 **of 177 bioactive-leads were identified displaying MIC <10 μM against H37Rv and selectivity**
271 **(therapeutic) index (SI = HepG2IC₅₀/MIC) \geq 50. These values are of the same order of magnitude of**
272 **those displayed by 4 (MIC = 0.13 μM and SI = 30), thus qualifying this compound as a promising**
273 **lead that can be improved in subsequent medicinal chemistry work.**

274 In addition, compounds **5, 7, 9, 10** and **12**, which exhibited the second best growth inhibitory activity
275 of the series against the TB causing bacillus (MIC = 0.16 mg/L), all contained at least one pyrrole ring
276 in their three-heterocyclic chains. PBD-conjugates with three-imidazole (**8**) and three-thiazole (**11**)

277 chains showed a 2-fold and 30-fold decrease in *M. tuberculosis* growth inhibitory activity,
278 respectively. This study also showed that the antimicrobial activity of PBD-conjugates **1-12** was
279 highly selective against slow-growing mycobacteria *M. tuberculosis* and *M. bovis* compared to fast-
280 growing bacteria *E. coli*, *P. putida* and *Rhodococcus sp.* The mechanism of action of the PBDs is
281 unique and involves the covalent binding to guanine residues within the DNA minor-groove. The
282 DNase I footprinting results showed that the PBD-conjugates bound with high affinity to large DNA
283 sequences containing short A/T stretches followed by a guanine residue, with **9** protecting the 5'-
284 TAAACGTT sequence at a concentration as low as 0.5 μ M. This can be exploited to target discrete
285 DNA sequences within the GC-rich mycobacterial genome and ultimately disrupt key enzymes and
286 transcription factors. DNA melting studies revealed that thiazole-containing **9**, and to a lesser extent
287 **10**, formed strong complexes and markedly shifted the melting curves of the two 14-mer DNA
288 duplexes used in this study, thus confirming the significant DNA stabilisation properties of the
289 compounds. In summary, these results show that **1-12** could serve as DNA-targeted therapeutic leads
290 for the treatment of tuberculosis and further studies are underway to implement the potency and
291 therapeutic index of these compounds.

292 **Acknowledgements**

293 We thank Professor Siamon Gordon for providing the RAW264.7 cell-line and Professor Simon Croft
294 for granting access to the TB lab in the LSHTM. SB is a Cipla Distinguished Fellow in
295 Pharmaceutical Sciences. Supported by MRC, UK (Grant Code: G0801956 to S.B.) to fund D.E. and
296 T.M.'s post-doctoral studies at Birkbeck, University of London. J.D.G. received financial support
297 from Colfuturo and a Bloomsbury Colleges studentship for his PhD studies. E.M. carried out a PhD
298 rotation in S.B.'s lab funded by a Wellcome Trust Scholarship. M.A.B. is a Commonwealth Scholar
299 in K.R.F.'s lab. The funders had no role in study design, data collection and analysis, decision to
300 publish or preparation of the manuscript.

301 **References**

302 1. WHO. Global tuberculosis report 2012. Geneva: WHO. (2014)

- 303 2. Guzman JD, Gupta A, Bucar F, Gibbons S, Bhakta S. Antimycobacterials from natural
304 sources: ancient times, antibiotic era and novel scaffolds. *Front Biosci.* 17:1861-1881 (2012)
- 305 3. Galagan JE, et al. The Mycobacterium tuberculosis regulatory network and hypoxia. *Nature.*
306 499(7457):178-183 (2013)
- 307 4. Denny WA, Abraham DJ. Synthetic DNA-Targeted Chemotherapeutic Agents And Related
308 Tumor-Activated Prodrugs. *In Burger's Medicinal Chemistry and Drug Discovery.* John
309 Wiley & Sons, Inc., (2003)
- 310 5. Cozzi P, Mongelli N, Suarato A. Recent anticancer cytotoxic agents. *Current medicinal*
311 *chemistry. Anti-cancer agents.* 4(2):93-121 (2004)
- 312 6. Hartley JA, Hochhauser D. Small molecule drugs - optimizing DNA damaging agent-based
313 therapeutics. *Current opinion in pharmacology.* 12(4):398-402 (2012)
- 314 7. Baraldi PG, et al. DNA minor groove binders as potential antitumor and antimicrobial agents.
315 *Med Res Rev.* 24(4):475-528 (2004)
- 316 8. Hartley JA. The development of pyrrolobenzodiazepines as antitumour agents. *Expert opinion*
317 *on investigational drugs.* 20(6):733-744 (2011)
- 318 9. Antonow D, Thurston DE. Synthesis of DNA-interactive pyrrolo[2,1-c][1,4]benzodiazepines
319 (PBDs). *Chemical reviews.* 111(4):2815-2864 (2011)
- 320 10. Leimgruber W, Stefanovic V, Schenker F, Karr A, Berger J. Isolation and characterization of
321 anthramycin, a new antitumor antibiotic. *Journal of the American Chemical Society.*
322 87(24):5791-5793 (1965)
- 323 11. Antonow D, et al. Solution structure of a 2:1 C2-(2-naphthyl) pyrrolo[2,1-
324 c][1,4]benzodiazepine DNA adduct: molecular basis for unexpectedly high DNA helix
325 stabilization. *Biochemistry.* 47(45):11818-11829 (2008)
- 326 12. Puvvada MS, et al. Inhibition of bacteriophage T7 RNA polymerase in vitro transcription by
327 DNA-binding pyrrolo[2,1-c][1,4]benzodiazepines. *Biochemistry.* 36(9):2478-2484 (1997)
- 328 13. Hartley JA, et al. SG2285, a novel C2-aryl-substituted pyrrolobenzodiazepine dimer prodrug
329 that cross-links DNA and exerts highly potent antitumor activity. *Cancer research.*
330 70(17):6849-6858 (2010)
- 331 14. Hartley JA, Hamaguchi A, Suggitt M, Gregson SJ, Thurston DE, Howard PW. DNA
332 interstrand cross-linking and in vivo antitumor activity of the extended pyrrolo[2,1-
333 c][1,4]benzodiazepine dimer SG2057. *Investigational new drugs.* 30(3):950-958 (2012)
- 334 15. Rahman KM, et al. Antistaphylococcal activity of DNA-interactive pyrrolobenzodiazepine
335 (PBD) dimers and PBD-biaryl conjugates. *Journal of Antimicrobial Chemotherapy.*
336 67(7):1683-1696 (2012)
- 337 16. Rosado H, Rahman KM, Feuerbaum E-A, Hinds J, Thurston DE, Taylor PW. The minor
338 groove-binding agent ELB-21 forms multiple interstrand and intrastrand covalent cross-links
339 with duplex DNA and displays potent bactericidal activity against methicillin-resistant
340 *Staphylococcus aureus.* *Journal of Antimicrobial Chemotherapy.* 66(5):985-996 (2011)
- 341 17. Rahman KM, et al. GC-Targeted C8-Linked Pyrrolobenzodiazepine-Biaryl Conjugates with
342 Femtomolar in Vitro Cytotoxicity and in Vivo Antitumor Activity in Mouse Models. *J. Med.*
343 *Chem.* 56(7):2911-2935 (2013)
- 344 18. Hadjivassileva T, Thurston DE, Taylor PW. Pyrrolobenzodiazepine dimers: novel sequence-
345 selective, DNA-interactive, cross-linking agents with activity against Gram-positive bacteria.
346 *Journal of Antimicrobial Chemotherapy.* 56(3):513-518 (2005)
- 347 19. Pepper CJ, Hambly RM, Fegan CD, Delavault P, Thurston DE. The novel sequence-specific
348 DNA cross-linking agent SJG-136 (NSC 694501) has potent and selective in vitro
349 cytotoxicity in human B-cell chronic lymphocytic leukemia cells with evidence of a p53-
350 independent mechanism of cell kill. *Cancer research.* 64(18):6750-6755 (2004)
- 351 20. Antonow D, Jenkins TC, Howard PW, Thurston DE. Synthesis of a novel C2-aryl
352 pyrrolo[2,1-c][1,4]benzodiazepine-5,11-dione library: effect of C2-aryl substitution on
353 cytotoxicity and non-covalent DNA binding. *Bioorganic & medicinal chemistry.* 15(8):3041-
354 3053 (2007)
- 355 21. Brucoli F, et al. An extended pyrrolobenzodiazepine-polyamide conjugate with selectivity for
356 a DNA sequence containing the ICB2 transcription factor binding site. *J Med Chem.*
357 56(16):6339-6351 (2013)

- 358 22. Brucoli F, et al. Novel C8-linked pyrrolbenzodiazepine (PBD)-heterocycle conjugates that
359 recognize DNA sequences containing an inverted CCAAT box. *Bioorganic & medicinal*
360 *chemistry letters*. 21(12):3780-3783 (2011)
- 361 23. Wells G, et al. Design, synthesis, and biophysical and biological evaluation of a series of
362 pyrrolbenzodiazepine-poly(N-methylpyrrole) conjugates. *J Med Chem*. 49(18):5442-5461
363 (2006)
- 364 24. Dervan PB. Molecular recognition of DNA by small molecules. *Bioorganic & medicinal*
365 *chemistry*. 9(9):2215-2235 (2001)
- 366 25. Brucoli F, Guzman JD, Maitra A, James CH, Fox KR, Bhakta S. Synthesis, anti-
367 mycobacterial activity and DNA sequence-selectivity of a library of biaryl-motifs containing
368 polyamides. *Bioorganic & Medicinal Chemistry*. 23(13):3705-3711 (2015)
- 369 26. Guzman JD, et al. Antitubercular specific activity of ibuprofen and the other 2-arylpropanoic
370 acids using the HT-SPOTi whole-cell phenotypic assay. *BMJ Open*. 3(6) (2013)
- 371 27. Danquah CA, Maitra A, Gibbons S, Faull J, Bhakta S. HT-SPOTi: A Rapid Drug
372 Susceptibility Test (DST) to Evaluate Antibiotic Resistance Profiles and Novel Chemicals for
373 Anti-Infective Drug Discovery. *Current protocols in microbiology*. 40:17 18 11-17 18 12
374 (2016)
- 375 28. Hampshire AJ, Fox KR. Preferred binding sites for the bifunctional intercalator TANDEM
376 determined using DNA fragments that contain every symmetrical hexanucleotide sequence.
377 *Analytical biochemistry*. 374(2):298-303 (2008)
- 378 29. Ballell L, et al. Fueling Open-Source Drug Discovery: 177 Small-Molecule Leads against
379 Tuberculosis. *Chemmedchem*. 8(2):313-321 (2013)

380

381

382

383 **Figure Legends**

384

385 **Figure 1.** Schematic representation of the mechanism of action of PBDs involving the nucleophilic
386 attack of the C2-NH₂ group of a guanine residue to the N10-C11 imine moiety of PBD within the
387 DNA minor groove.

388

389 **Figure 2.** The library of twelve C8-linked PBD-heterocyclic polyamide conjugates **1-12** tested in this
390 study.

391

392 **Figure 3.** DNase I footprinting patterns of the PBD-conjugates on the HexBrev and HexAfor DNA
393 fragments. The first two panels show the results in the presence of 10 μM of each of the PBD-
394 conjugates. The second two panels show the concentration dependence of footprints on HexAfor with
395 **5** and **9**. Ligand concentrations (μM) are shown above each gel lane. The bars indicate the location
396 of clear footprints. Tracks labelled GA are sequence markers specific for G and A, while con
397 indicates DNase I cleavage in the absence of added ligand.

398

399 **Figure 4.** Sequences of HexAfor and HexBrev indicating the location of binding sites of the PBD-
400 conjugates (underlined and numbered in sequences).

401

402 **Figure 5.** Fluorescence melting profiles for the DNA duplexes 5'-F-AAAAGGATCCAAAA/5'-
403 TTTTGGATCCTTTT-Q and 5'-F-AAAAGTATACAAAA/5'-TTTTGTATACTTTT-Q (F =
404 fluorescein and Q = dabcy). The ligand concentration was 0.5 μM with 0.25 μM target duplex.

405

406

407

408

409

410

411

412

413

414

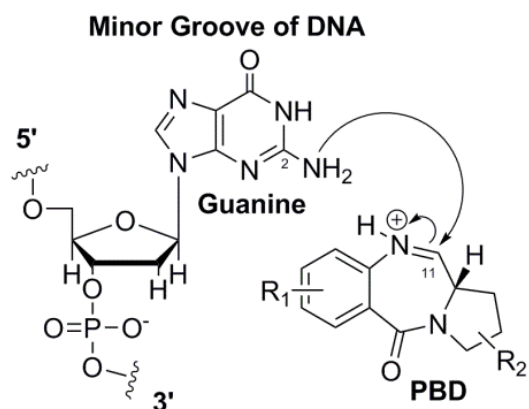
415

416 **Figures**

417

418

419 **Figure 1**



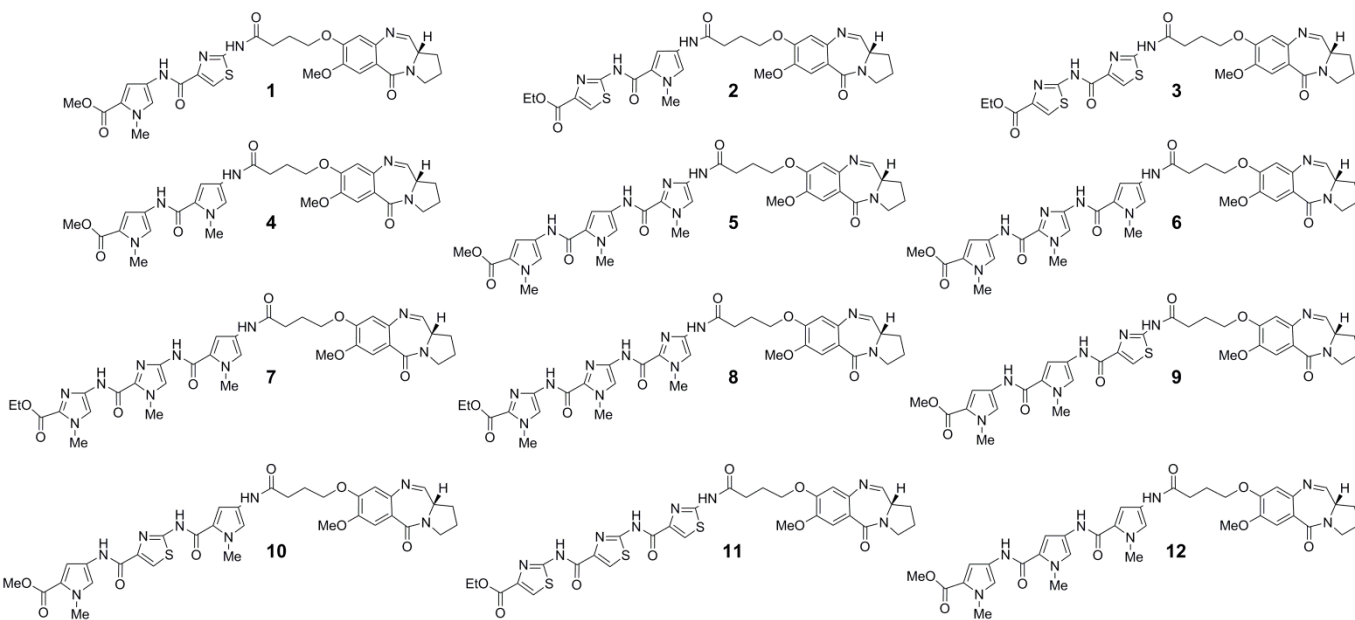
420

421

422

423

424 **Figure 2**



425

426

427

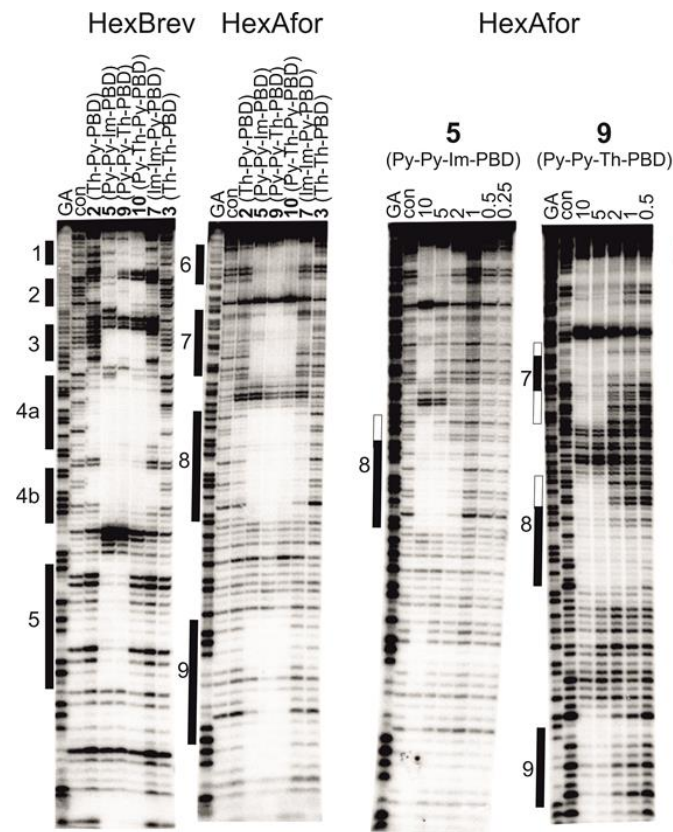
428

429

430

431

432 **Figure 3**



433

434

435

436

437

438 **Figure 4**

439

HexBrev

5'-...GGATCCATGCATT AATTCGAATATTGATCATGACGTCTGACA TGTACATATGTATATACG
1 2

CGCGTACGC GTATACGTAGCGCGCTT ATAAGCTTGCAATTGCCGGCT AATTAGGGCCCTC
3 4a 4b

GAGCTCGCGATCGGCCGGATCC-3'
5

HexAfor

5'-...GGATCCCGGGATATCGATATA TGGCGCCAAATTTAGCTATAGATCTAGAATTCCGGACC
6

GCGGTTTAAACGTTAACCGGTACCTAGGCCTGCAGCTGC GCATGCTAGCGCTTAAGTACTAG
7 8

TGCACGTGGCCA TGGATCC-3'
9

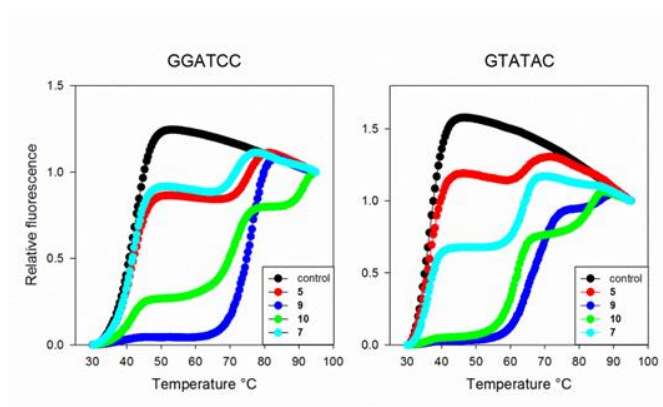
440

441

442

443

444 **Figure 5**



445

446

447

448

449

450

451

452

453

454

455

456

457

458

459

460

461

462

463

464

465

466

467

468

469

470

471

472 **Tables**

473

474 **Table 1.** Biological activity of PBD-conjugates **1-12**.

Compound	MICs (mg/L)					GIC ₅₀ RAW264.7 (mg/L)	SI ^a
	<i>Mycobacterium tuberculosis</i> H ₃₇ Rv	<i>Mycobacterium bovis</i> BCG	<i>Escherichia coli</i> K12	<i>Pseudomonas putida</i> KT2442	<i>Rhodococcus sp.</i> RHA1		
Py-Th-PBD (1)	0.31	0.16	1.25	>20	1.25	4.45	14.4
Th-Py-PBD (2)	0.63	0.63	2.5	>50	5.0	2.41	3.83
Th-Th-PBD (3)	5.19	<20	>50	>50	>50	2.41	0.46
Py-Py-PBD (4)	0.08	0.04	1.25	10.0	1.25	2.41	30.1
Py-Py-Im-PBD (5)	0.16	0.16	1.25	10.0	1.25	1.66	10.4
Py-Im-Py-PBD (6)	0.32	<20	1.25	50.0	1.25	1.66	5.19
Im-Im-Py-PBD (7)	0.16	0.08	1.25	>50	1.25	1.66	10.4
Im-Im-Im-PBD (8)	0.32	<20	50.0	>50	10.0	1.66	5.19
Py-Py-Th-PBD (9)	0.16	0.08	1.25	50.0	1.25	1.66	10.4
Py-Th-Py-PBD (10)	0.16	0.08	1.25	>50	1.25	1.66	10.4
Th-Th-Th-PBD (11)	5.19	ND	>50	>50	>50	1.66	0.32
Py-Py-Py-PBD (12)	0.16	0.04	1.25	5.0	1.25	1.66	10.4
Isoniazid	0.05	0.05	ND	ND	ND	3000	60000
Rifampin	0.05	0.05	ND	ND	ND	700	14000
Kanamycin	ND	ND	1.0	1.0	10.0	ND	ND

475 ^aThe SI was calculated by dividing the GIC₅₀ for RAW264.7 by the MIC against *M. tuberculosis* H₃₇Rv

476

477

478

479 **Table 2.** Changes in melting temperature (ΔT_m) of the oligonucleotide duplexes in the presence of 0.5 μ M of each ligand and

480 the fraction of the transition that corresponds to the uncomplexed duplex.

	GGATCC $T_m = 41.7$ °C		GTATAC $T_m = 36.4$ °C	
	ΔT_m	% free	ΔT_m	% free
Py-Py-Im-PBD (5)	33	75	28	80
Im-Im-Py-PBD (7)	30	80	28	55
Py-Py-Th-PBD (9)	35	10	29	5
Py-Th-Py-PBD (10)	31	25	26	0

481

482

483

